VOL. 13, NO. 13, JULY 2018 ISSN 1819-6608
ARPN Journal of Engineering and Applied Sciences
©2006-2018 Asian Research Publishing Network (ARPN). All rights reserved.
www.arpnjournals.com

A THREE DIMENSIONAL FOOT FOURIER DESCRIPTORS MODEL

Omar bin Mohd Rijal[1], Mohd Faizal Mohd Hamzah[2], S. Sankaraiah[1] and Norliza Mohd Noor[2]
[1]Institute of Mathematical Sciences, Faculty of Science, University of Malaya, Lembah Pantai, Kuala Lumpur Malaysia
[2]Razak School of UTM Engineering and Advanced Technology, Universiti Teknologi Malaysia, UTM Kuala Lumpur Campus, Jalan Sultan Yahya Petra, Kuala Lumpur, Malaysia
E-Mail: norliza@utm.my

ABSTRACT

Knowledge of the 3D foot shape is important for the shoe industry, in particular, to provide comfort and fit to the users. In this study a random sample of 150 Malaysian adult women aged 19-60 years feet were scanned using the Infoot scanner system. Fourier Descriptor (FD) was then used to reconstruct a new model, with additional properties, and labeled as the FD foot model from the 3D homologous model. Six similarity measures and the Bland-Altman plot showed that the 3D FD foot model is almost identical to the 3D homologous model. Measurements of foot length, foot width and ball girth from both types of models were found to be almost identical. The FD terms was then showed to have a complex normal probability distribution which allows a way of quantifying the variability of individual points. This knowledge will be of great use for the shoe industry.

Keywords: shape model, women's foot, Fourier descriptor, complex normal.

INTRODUCTION

In the past, shoe manufacturers depend solely on empirical values obtained from technicians, later which are passed on from generation to generation [1, 2]. However, technology advancement in the recent years has enabled the development of algorithms for matching 3D objects such as feet and lasts. These algorithms unfortunately are barely suitable to account for a subject-specific feel of fit [3]. Although direct comparisons of foot and last measures are difficult to generalize, grading of a shoe last should be identical to the grading of real feet. A complex grading system determines how a last progresses from size to size. With each change in size, all other foot dimensions also change in a systematic manner. These are two kinds of grading for lasts, either obtaining lasts for different foot length (length grading), or obtaining lasts for different ball girth or foot breadth with the same foot length (girth grading). These grading rules can differ between last manufacturers and brands.

The characteristic of foot shape is manifold, since numerous factors are associated with foot morphology. Aside from natural biological variance, distinctive age classes and population groups show prevalent qualities in foot dimensions [4, 5]. Furthermore, differences in foot shape are also influenced by factors such as body mass index (BMI), parity, and sex [6]. In order to ensure proper shoe fit for the majority of population, classification of foot types should be carried out [7, 8].

Three-dimensional foot modeling is important in order to evaluate foot measurements and volume quickly and accurately, especially in the medical and industrial applications such as to evaluate efficacy of treatments of various foot problem [9 - 11] and for inner space estimation of shoe-making [12, 13]. There are many 3-D scanning technology available with very high accuracy that have been used widely in foot researches [14 - 18]. Fundamental to the foot problems suggested above there is a clear need to be able to represent and measure accurately the shape of the foot. Existing shape representation depends on appropriate selection of foot dimensions which raises the questions of which shape model to select. For instance, on the focus on foot surface area has resulted in numerous regression models as possible candidates [19 - 23]. A similar situation arises when the focus is on foot volume [11].

Fourier Descriptors (FD) is a contour-based approach where all points are connected to describe the shape [24-25]. It can use as discrete approach (structural) where each segment of the shape is taken independently or continuous approach (global) where the shape is taken as a whole [24]. FD is proven to be translation, scale and rotation invariant [25], and certain Fourier descriptors are shearing invariant [27]. It has many nice characteristics, namely, simple derivation, simple normalization, simple to do matching, robust to noise, perceptually meaningful, compact and hierarchical coarse to fine representation [26]. As a shape descriptor, FD has proved to have good retrieval accuracy, compact features, general application, low computation complexity and robust retrieval performance [24, 28]. By using the Fourier coefficient, the shape contour can be represented by fewer numbers of Fourier coefficients that resulted in data reduction [25].
The aim of this study is to reconstruct the 3D foot homologous model obtained from Infoot scanner system using Fourier Descriptors. The FD terms investigated is found to be closely represented the 3D foot homologous model. The FD terms have complex normal probability distribution that is useful in the shoe industry where foot shape feature can be quantify.

MATERIAL AND METHODS

Data collection

The University Malaya ethical committee approved this study. All volunteers signed the consent form provided before the scanning process. A total of 150 volunteers of the 150 Malaysian adult women aged between 19 to 60 years old from students and staff of

©2006-2018 Asian Research Publishing Network (ARPN). All rights reserved.

University of Malaya participated in the study. None of them had any visible foot abnormalities and their ages, body weight and height are given in Table-1. The foot shape measurements of the volunteers were obtained using a "3D Infoot scanner" from I-Ware Laboratory, Japan.

Table-1. Summary statistics of the samples' height, body weight and age.

	Height (cm)	**Body weight** (kg)	**Age**
Mean	157.62	59.02	27.946
Standard Deviation	7.09	15.74	8.666

The 2D and 3D foot measurements of these women were collected using INFOOT USB scanning system (I-Wave Laboratory Co., Ltd, Japan). Di+ is software developed by I-Wave Laboratory Co., Ltd, Japan, which generates homologous foot model. To generate the 3D foot homologous model requires foot shape data and five additional landmark positions on the tip of the toes. These additional landmarks were manually placed using Landmark Editing interface in D+ software as shown in Figure-2 and Figure-3. The new landmarks placed 3D foot data is saved as .fbd file.

After modeling, 3D mesh data is generated and saved as .geo file. The final foot model is saved in database with the file name. The homologous foot model and its corresponding 13 cross sections which consists of 295 points are shown in Figure-4 and Figure-5, respectively.

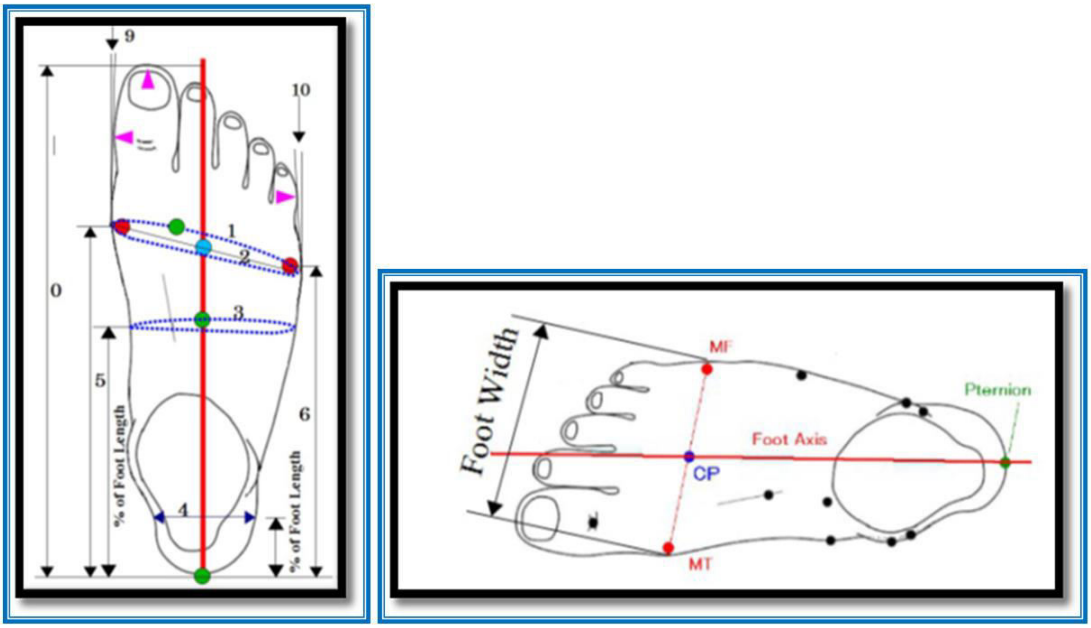

Figure-1. The image illustrate the five foot measurements obtained from I-Ware USB High Type Foot Scanner with foot length (0), ball girth circumference (1), foot width (2), instep length (5), and fibulare instep length (6).

©2006-2018 Asian Research Publishing Network (ARPN). All rights reserved.

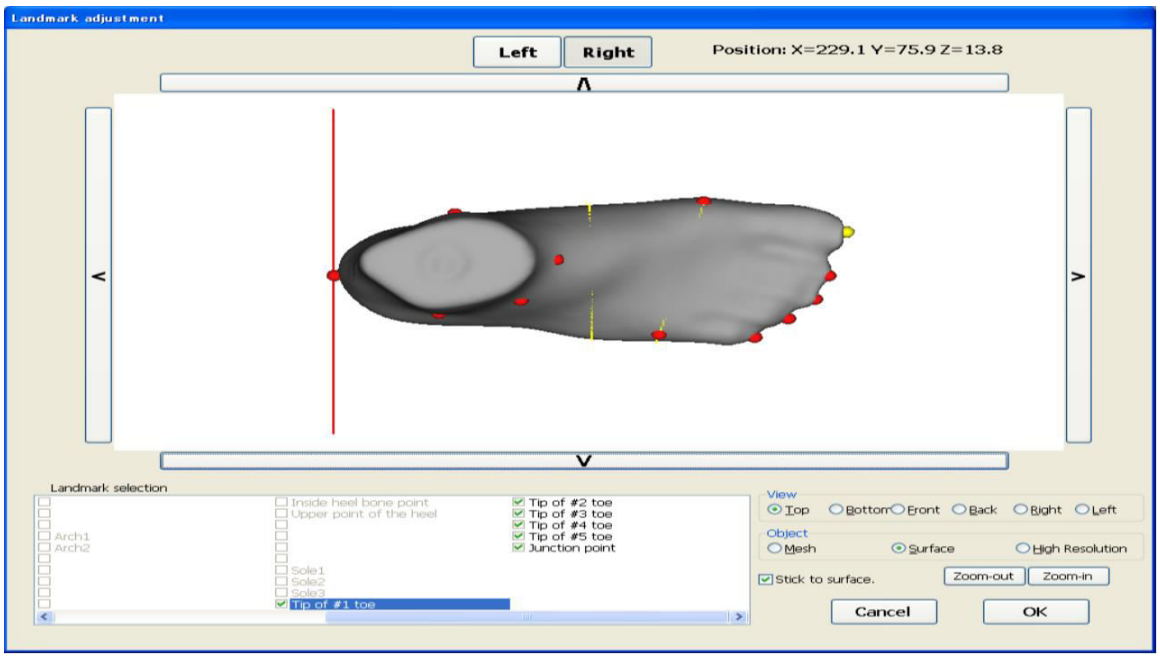

Figure-2. Additional landmarks placed onto the tip of five toes.

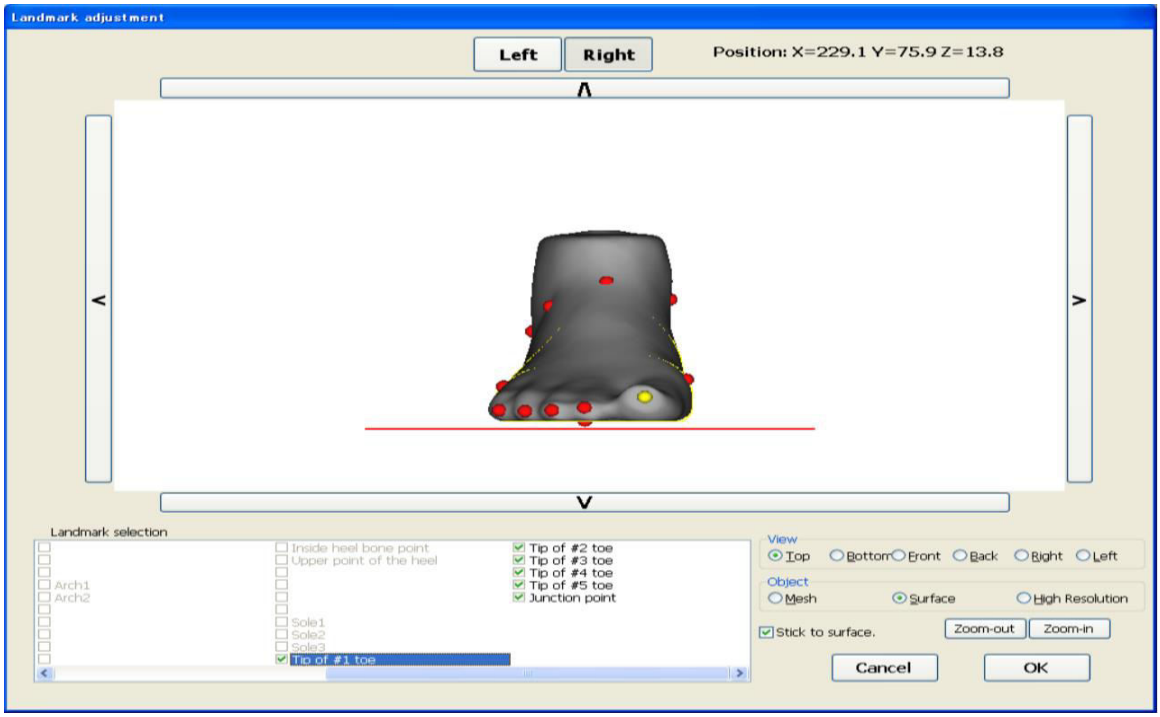

Figure-3. Front view of the right foot to confirm all placements of land marks.

©2006-2018 Asian Research Publishing Network (ARPN). All rights reserved.

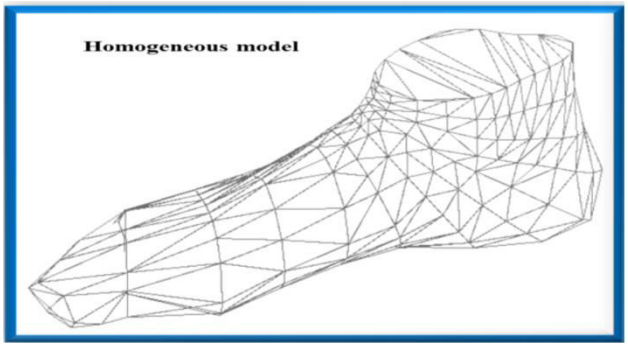

Figure-4. The 3D foot homologous model.

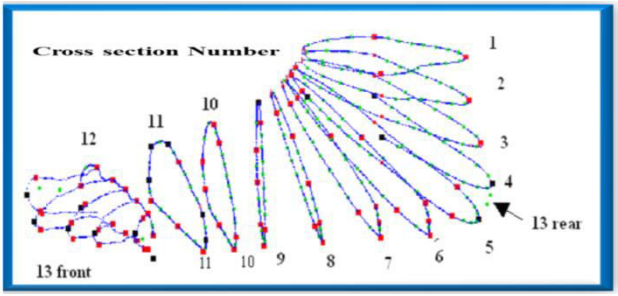

Figure-5. The thirteen cross sections consisting of 295 points.

Experimental setup

The anatomy of each foot is marked using the sticker label. Land marking is an essential process in getting accurate measurement when using the Infoot scanner system. The volunteer is required to stand with one foot on the scanning platform and the other outside the scanning area. The volunteer must stand at ease with the body weight equally distributed on both feet. Each scanning was done twice for the first 60 volunteers and the difference $w_i = w_i^{(1)} - w_i^{(2)}$, $i = 1,\ldots,60$ of the two measurements on the same individual were obtained. The Technical Error Measurement (TEM) which is use to determine intra-observer error to show consistency between two samples according to ISO 20685:2010 [29] is defined as $\sqrt{\frac{\sum_{i=1}^{N} w_i^2}{2N}}$. Small TEM values less than 2 mm for foot dimensions which is the maximum allowable error may be regarded as accurate measurements obtained from the experiment [30, 31]. Figure-1 shows the five measurements that were used in calculating TEM.

The Bland-Altman plot is the plot of points $\left\{\left(\frac{w_i^{(1)} + w_i^{(2)}}{2}\right), \left(w_i^{(1)} - w_i^{(2)}\right)\right\}$ where $i = 1,\ldots,60$ [32]. Consistent measurements by observer are shown when the points are close to the zero values along the horizontal axis and within the limit $\bar{w} \pm 2\text{SD}$, where $\bar{w}$ and SD are the sample mean and sample standard deviation of w_i values respectively.

FOURIER DESCRIPTOR

2D Fourier descriptor

Mathematical properties of Fourier descriptors (FD) allow the FD model to be robust and invariant with respect to translation, rotation and scale changes [33]. Let $(x(k), y(k))$ $k = 1,\ldots,N$ be the points, on a two dimensional object boundary. Let $s(k) = x(k) + jy(k)$, where k = 0, 1,…, N-1 and $j = \sqrt{-1}$. The discrete Fourier transform (DFT) of $s(k)$ yields

$$a_u = \frac{1}{N}\sum_{k=0}^{N-1} s(k)\exp\left(\frac{-j2\pi uk}{N}\right) \quad (1)$$

for $u = 0,1,\ldots,N-1$, [34]. The complex coefficients

$$a_u = c_u + jd_u \quad (2)$$

are known as the Fourier descriptors (FD) of the boundary. The set of FD for each object boundary was denoted as $\mathbf{A}_i = [a_0^i, a_1^i, \ldots, a_{N-1}^i]$, $i = 1,\ldots,n$, where n is the sample size.

The inverse Fourier transform of these coefficients restores $s(k)$, as given by,

$$s(k) = \sum_{u=0}^{N-1} a_u \exp\left(\frac{j2\pi uk}{N}\right) \quad (3)$$

for $k = 0,1,\ldots,N-1$.

3D Fourier Descriptor Foot Model

One hundred and fifty 3D right foot and 150 3D left foot homologous model were then subjected to Fourier transform. Each of the 3D foot homologous models consists of 295 points as shown in Figure-5(b). The 3D homologous model using 295 points was reproduced in MATLAB as sown in Figure-6.

©2006-2018 Asian Research Publishing Network (ARPN). All rights reserved.

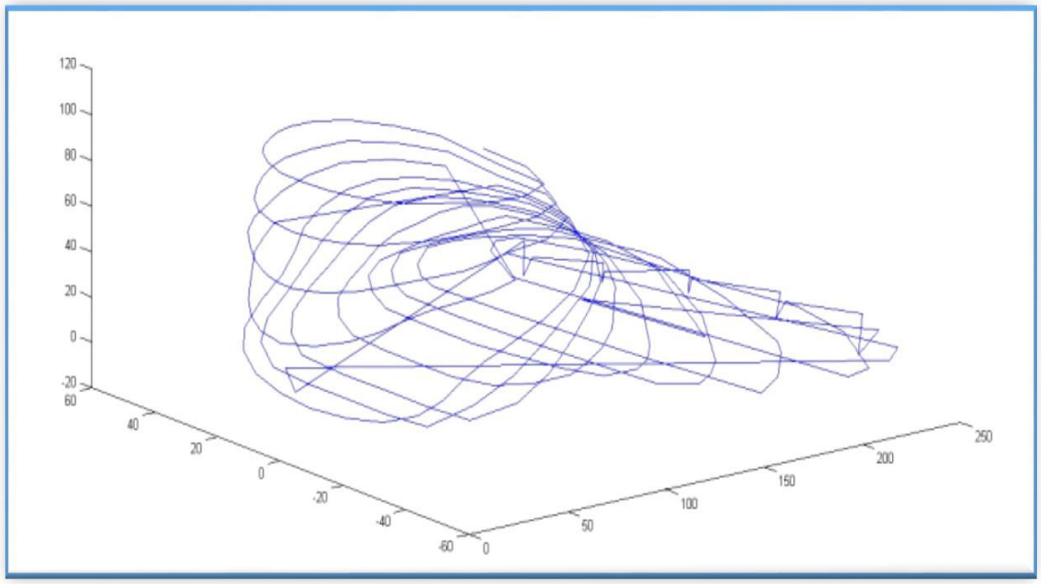

Figure-6. The reproduction of 3D foot homologous model in MATLAB.

The 3D discrete Fourier transform for the 3D coefficients $f(l,m,n)$ are represented as shown in Equation 4.

$$F[x,y,z]=\frac{1}{LMN}\sum_{l=0}^{L-1}\sum_{m=0}^{M-1}\sum_{n=0}^{N-1}f(l,m,n)\exp(-i2\prod(\frac{xl}{L}+\frac{ym}{M}+\frac{zn}{N})) \quad (4)$$

In order to restore 3D coefficients $f(l,m,n)$, the 3D inverse Fourier transform is represented as shown in Equation 5.

$$f(l,m,n)=\sum_{x=0}^{L-1}\sum_{y=0}^{M-1}\sum_{z=0}^{N-1}F[x,y,z]\exp(i2\prod(\frac{xl}{L}+\frac{ym}{M}+\frac{zn}{N})) \quad (5)$$

3D Fourier descriptors from can be computed by separating the 3D image plane to three 2D planes, i.e., *xy*, *yz* and *xz* planes for easier and faster computation. Once the individual 2D planes FD's are obtained as in Section 2.5, then all the three 2D planes FD's are combined to form 3D FD's using MATLAB function '*combine*'. This allows an individual foot that was represented by the set of 295 three dimensional points to be transform to a *q*-dimensional vector of FD (*q*< 295), see Table-2. The Procrustes distance initially determines an optimal q value, which will then be verified by Dice and Jaccard indices.

Procrustes distance

Following the notation of Section 2.4, the *N* points ($\mathbf{x}_r^o, r=1,2,\square,N$) obtained from the *q* Fourier descriptors, *q*<*N*, will be compared with the N-points $\mathbf{x}_r^m, r=1,2,\square,N$, when all the a_u terms were considered. The Procrustes distance (PD), PD_i = $\sum_{r=1}^{N}(\mathbf{x}_r^o-\mathbf{x}_r^m)'(\mathbf{x}_r^o-\mathbf{x}_r^m)$, can be used as a similarity measure [35, 36]. The optimal choice of *q* is that value of *q* that minimizes PD_i.

Similarity measures

In order to find the similarity between the foot shape represented using Fourier descriptors and the actual shape represented using 295 points obtained from the homologous model, the Procrustes distance, Dice similarity index, Jaccard similarity index, Relative Volume Difference (RVD) and Volume overlap error (VOE) measures are used. The Procrustes distance uses the Euclidean distance measure between vectors. The remaining similarity measures compares the volume of the 3D homologous foot model with 295 points represented by *A* and the volume of the 3D foot model represented with 154 FD points represented by *B*.

The volume can be determined using Delaunay triangulation formed from the 3D points as shown in using the Equation 6 [37]. A set of 3D points can be divided into triangles by connecting the data points as the vertices of these triangles.

$$Volume=\tfrac{1}{2}[x_1(y_2-y_3)+x_2(y_3-y_1)+x_3(y_1-y_2)]\frac{(z_1+z_2+z_3)}{3} \quad (6)$$

Where, $(x_1,y_1),(x2,y2),(x_3,y3)$ are the planar co-ordinates of the triangle vertices and z_1, z_2 and z_3 are the corresponding thickness between geological horizon.

The complex normal distribution

Very often selected cross section of the homologous model (or FD model), as shown in Figure-5(b), is of interest. Statistical variability of individual

©2006-2018 Asian Research Publishing Network (ARPN). All rights reserved.

points, $s(k)$ in equation (3), Section 2.4 is a way of quantifying variability of cross-sectional shapes.

Since each point $s(k)$ may be defined by q-FD terms, it correspond to having q- c_u terms and q-d_u terms (Equation 2, Section 2.4). The Kolmogorov-Smirnov test statistic, $D_n = \sup_x |F_n(x) - F_o(x)|$

Where, $F_n(x)$ is the cumulative distribution function (cdf) of the c_u-terms and $F_o(x)$ is the cdf of the hypothesized distribution function [38]. The value of D_n and its corresponding critical value (CV) were calculated for four points, a point on a toe, a point on a ball girth, a point on the heel and a point on the ankle. These calculations were then repeated for the d_u terms. In particular, the complex coefficients, a_u, is said to have a complex normal distribution if the c_u terms and d_u terms are normally distributed.

The variation of shape

For completeness, the variation of shapemust be stated and this is done by seeking the probability of the $\mathbf{A}_i$. Since $\mathbf{A}_i = \mathbf{c}_i + j\mathbf{d}_i$ where $\mathbf{c}_i^T = (c_1, c_2, \ldots, c_n)$, and $\mathbf{d}_i^T = (d_1, d_2, \ldots, d_n)$ therefore $\mathbf{A}_i$ has the well-known complex multi-normal probability distribution $CN(\mu, \Gamma, C)$ which can be described with three parameters;

$$\boldsymbol{\mu} = \mathrm{E}(\mathbf{A}_i) \tag{7}$$

$$\Gamma = \mathrm{E}[(\mathbf{A}_i - \boldsymbol{\mu})(\mathbf{A}_i^* - \boldsymbol{\mu}^*)^{\mathrm{T}}] \tag{8}$$

$$C = \mathrm{E}[(\mathbf{A}_i - \boldsymbol{\mu})(\mathbf{A}_i - \boldsymbol{\mu})^{\mathrm{T}}] \tag{9}$$

Where, $\mathbf{A}_i^T$ denotes matrix transpose and $\mathbf{A}_i^*$ denotes complex conjugate.

RESULTS

The results are presented in four sections, the first shows the reliability of observer measurement using the technical error measurement (TEM) and Bland-Altman plot. The second section showed the result of using Procrustes distance. The values of similarity indices when comparing the 3D 295 points homologous model with the proposed 3D FD model is in the third section. Finally, the existence of the complex normal distribution is investigated for the FD terms.

Reliability of Observer Measurement

Technical error measurement

The TEM for intra-observer error was carried over 60 samples where the scanning was done twice. The difference between the first reading and the second reading should be as small as possible to show consistency between two samples according to ISO 20685:2010 [24]. Table-2 shows the intra-observer error TEM. The results show the observer's consistent ability to accurately locate/ detect the landmarks. Table-3 shows Relative Technical Error of Measurement for Intra-observer. The observer produced low relative TEM which less than the maximum allowable error and this indicates a good precision in land marking.

Table-2. Intra-observer error for 60 samples.

Foot measurement	**TEM** (mm)	**Maximum allowable error** (mm)
Foot length (Right foot)	0.9569	2
Foot length (Left foot)	0.6551	2
Ball Girth circumference (Right foot)	1.3457	2
Ball Girth circumference (Left foot)	1.2540	2
Foot breadth (Right foot)	0.7799	2
Foot breadth (Left foot)	0.7898	2
Instep length (Right foot)	1.2600	2
Instep length (Left foot)	1.2716	2
Fibulare Instep length (Right foot)	1.0028	2
Fibulare Instep length (Left foot)	1.1311	2

©2006-2018 Asian Research Publishing Network (ARPN). All rights reserved.

Table-3. Relative Technical Error of Measurement for Intra-observer error.

Foot measurement	Relative TEM for Observer 1(%)
Foot length (Right foot)	0.4084
Foot length (Left foot)	0.2798
Ball Girth circumference (Right foot)	0.5916
Ball Girth circumference (Left foot)	0.5538
Foot breadth (Right foot)	0.8208
Foot breadth (Left foot)	0.8342
Instep length (Right foot)	0.7363
Instep length (Left foot)	0.7435
Fibulare Instep length (Right foot)	0.6585
Fibulare Instep length (Left foot)	0.7441

Bland and altman plot for intra-observer

This plot also allows us to investigate any possible relationship between the two measurements. From this plot, it is informative for us to assess the magnitude of disagreement, to spot outliers and to see if there is any trend, example, the increase of the difference for high values. Most differences on the y-axis are expected to lie within $\overline{w} \pm 2\text{SD}$ and these can be referred to "the limits of agreement" as illustrated by the grey region in Figure-7. Although a few outliers were detected the general results remains unaffected.

Most of the points in the Bland Altman plot lie within the range of ±2 standard deviation along the vertical axis indicating that the land-marking was accurately carried out. From the Bland Altman plots, the reliability is between 93.3% to 98.3%, which is shown in Table-4.

Finding the optimum 3D fourier descriptor foot model

The Procrustes distance when using *q*-FD terms compared to when using all FD-terms, as explained in Section 2.5, is illustrated in Figure-8 and Figure-9, for left and right foot respectively. For both left and right foot, the Procrustes distance no longer decreased and remained constant at almost zero value after 154 FD terms. This strongly suggests that 154 points on the proposed FD model is sufficient to represent the homologous model. Similarity measures were then used to verify this result.

Similarity measures

Dice similarity index (D), Jaccard similarity index (J), volume overlap Error (VOE) and Relative Volume Difference (RVD) are used to verify the results from Section 3.2. Table-5 and Table-6 illustrate the similarity measures between the proposed FD model and the 295 points homologous model. These results verify that 154 points of the FD model are sufficient to represent the 295 points 3D foot homologous model given the following observation: the Dice similarity index is 0.975 for left foot and 0.973 for right foot, the Jaccard similarity index is 0.976 for left foot and 0.974 for right foot, the VOE is 0.014 for left foot and 0.015 for right foot and the RVD is 0.000138 for left foot and 0.00015 for right foot.

Comparing measurements from model

A verification of the above result is the comparison of selected measurements, in particular, foot volume (FV), foot length (FL), foot width (FW) and ball girth (BG) for both the proposed FD model and the 3D homologous model. Table-7 and Table-8 show that univariate quantities, FL, FW and BG are almost identical for both the proposed FD model and the 3D homologous model. However, for the three-dimensional quantities, FV shows a slight difference.

Or a second verification, the Bland-Altman plot illustrates the consistency of volume measurement from both type of models. Figure-10 show foot volumes differences obtained from 3D FD model with 154 points and 3D homologous model for right and left foot. The majority of individuals studied are within the interval (-2SD, +2SD) suggesting consistency of volume measurement. However, a few individuals with small feet are outliers.

©2006-2018 Asian Research Publishing Network (ARPN). All rights reserved.

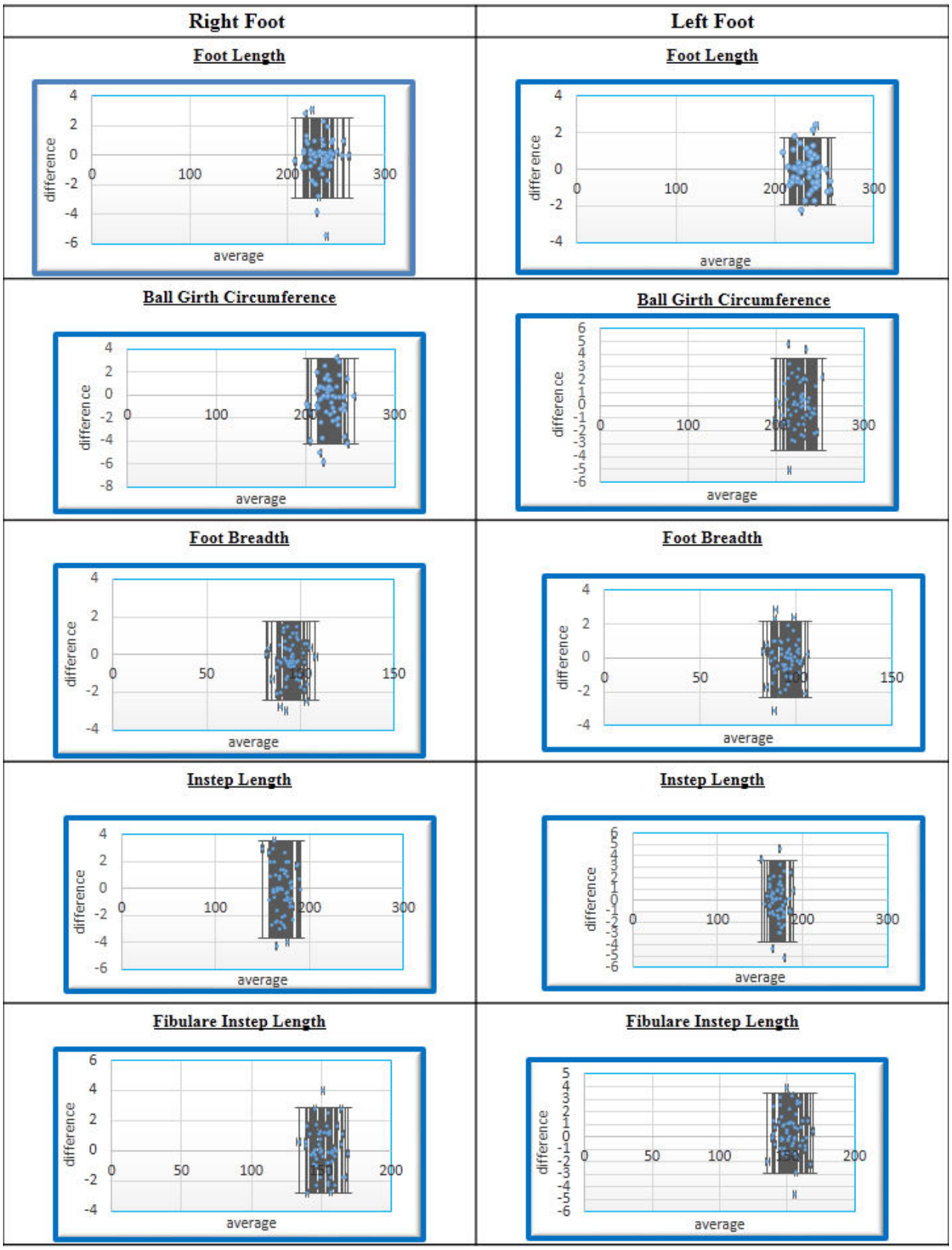

Figure-7. The Bland and Altman plots for intra-observer.

©2006-2018 Asian Research Publishing Network (ARPN). All rights reserved.

Table-4. The intra-observer reliability measure.

Foot measurement	**Intra-observer reliability** (%)
Foot length (Right foot)	93.3
Foot length (Left foot)	95.0
Ball Girth circumference (Right foot)	96.7
Ball Girth circumference (Left foot)	95.0
Foot breadth (Right foot)	96.7
Foot breadth (Left foot)	95.0
Instep length (Right foot)	96.7
Instep length (Left foot)	93.3
Fibulare Instep length (Right foot)	98.3
Fibulare Instep length (Left foot)	96.7

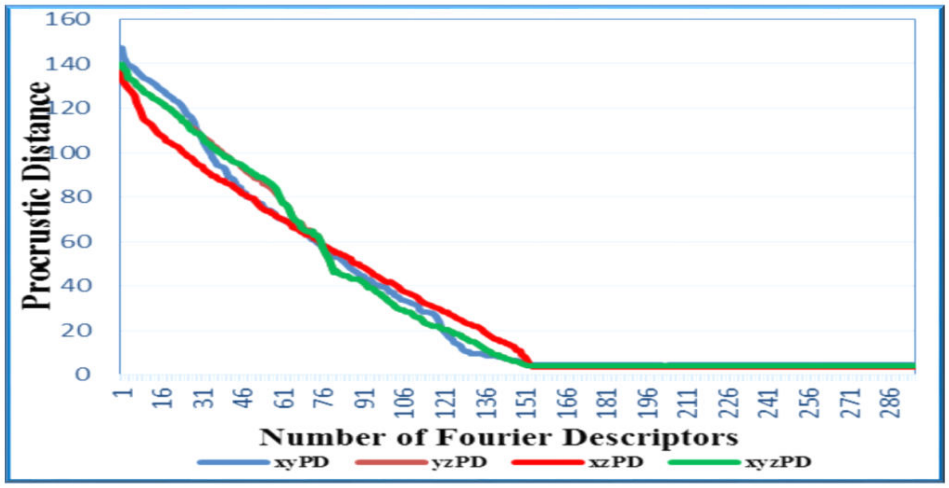

Figure-8. Left foot Procrustes distance variation with the number of Fourier Descriptors.

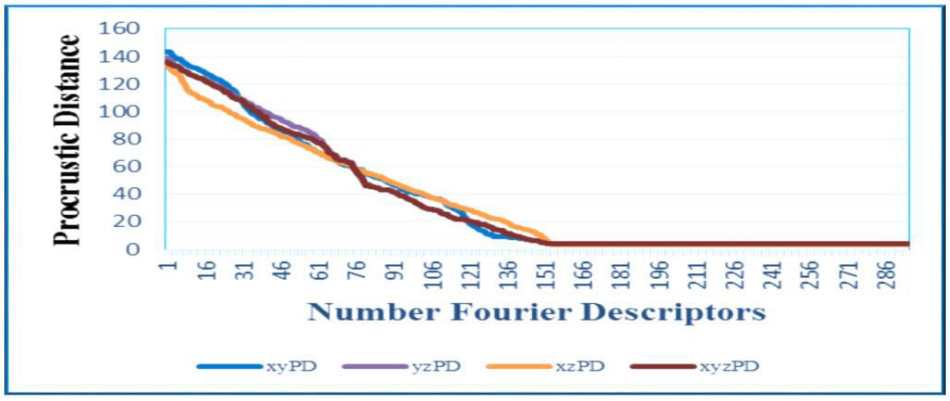

Figure-9. Right foot Procrustes distance variation with the number of fourier descriptors.

©2006-2018 Asian Research Publishing Network (ARPN). All rights reserved.

Table-5. Similarity Measures of volume from FD model relative to the homologous model for the left foot.

	Dice similarity index (D) **Mean** (SD)	**Jaccard similarity index**(J) **Mean** (SD)	**Volume overlap error** (VOE) **Mean** (SD)	**Relative Volume Difference** (RVD) **Mean** (SD)
50 Fourier Descriptors	0.274	0.195	0.805	0.0792
100 Fourier Descriptors	0.648	0.592	0.408	0.0428
154 Fourier Descriptors	0.975	0.976	0.014	0.000138
200 Fourier Descriptors	0.979	0.980	0.009	0.00001
250 Fourier Descriptors	0.983	0.983	0.006	0.00001
294Fourier Descriptors	0.996	0.995	0.002	0.00001

Table-6. Similarity Measures of volume from FD model relative to the homologous model for the right foot.

	Dice similarity index (D) **Mean** (SD)	**Jaccard similarity index**(J) **Mean** (SD)	**Volume overlap Error**(VOE) **Mean** (SD)	**Relative Volume Difference**(RVD) **Mean** (SD)
50 Fourier Descriptors	0.295	0.202	0.797	0.0738
100 Fourier Descriptors	0.667	0.602	0.374	0.493
154 Fourier Descriptors	0.973	0.974	0.015	0.00015
200 Fourier Descriptors	0.978	0.977	0.01	0.00001
250 Fourier Descriptors	0.985	0.982	0.009	0.00001
294 Fourier Descriptors	0.995	0.994	0.003	0.00001

Table-7. Left foot repeatability of the 3-D foot measurement system (unit: mm, mm^3) without outliers.

	3D FD model				**3D Homologous model**			
	Foot Volume (FV)	**Foot Length** (FL)	**Foot Width** (FW)	**Ball Girth** (BG)	**Foot Volume** (FV)	**Foot Length** (FL)	**Foot Width** (FW)	**Ball Girth** (BG)
Mean	830946	234.165	95.50	227.94	840072	233.841	95.179	227.916
STD	2395.73	0.16	0.11	0.47	2402.81	0.16	0.11	0.47

Table-8. Right foot repeatability of the 3-D foot measurement system (unit: mm, mm^3) without outlier.

	3D - 154 FD model				**3D Homologous model**			
	Foot Volume (FV)	**Foot Length** (FL)	**Foot Width** (FW)	**Ball Girth** (BG)	**Foot Volume** (FV)	**Foot Length** (FL)	**Foot Width** (FW)	**Ball Girth** (BG)
Mean	840015	233.188	95.56	228.34	840137	234.026	95.475	228.397
STD	2401.82	0.162	0.11	0.48	2409.37	0.16	0.12	0.48

©2006-2018 Asian Research Publishing Network (ARPN). All rights reserved.

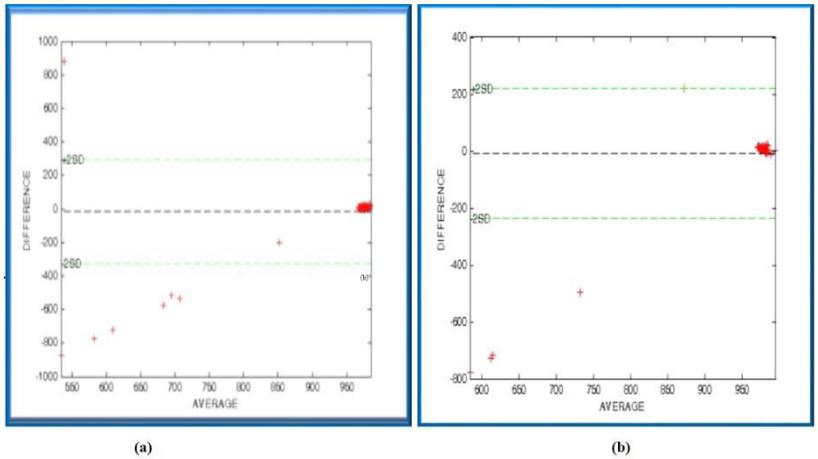

Figure-10. Bland-Altman plot showing differences for 150 right foot samples (a) and left foot samples (b) between 3D FD model with 154 FD points with 3D homologues model.

As an illustration of the appropriateness of the 154 FD model, its 3D representation is overlapped with the corresponding 3D homologous model. Figure-11(a) - (h) show different orientation of the foot strongly suggesting that 154 FD model is capable of capturing most of the details of the foot shape.

The complex normal distribution

The Kolmogorov-Smirnov (KS) test of normality is illustrated in Table-9 and Table-10. The four points, a point on the toe (T1), a point on the ball girth (T2), a point on the heel (T3), and a point on the ankle (T4) where chosen arbitrarily to represent the variety of position for points on the human foot. Since the KS statistics, D_n, is always less than the critical value (CV) for both c_u and d_u, this results strongly implies that the complex coefficients a_u in equation 2, Section 2.4 has the complex normal distribution. Henceforth, these results show that the point $s(k)$ in equation 3, Section 2.4 has a given probability distribution.

Table-9. The Kolmogorov-Smirnov test of normality for the c_u terms.

Real part variable FD (c_u)	**T1 CV=0.5102**	**T2 (CV=0.5081)**	**T3 (CV=0.4947)**	**T4 (CV=0.4908)**
D_n	0.215	0.202	0.204	0.194

Table-10. The Kolmogorov-Smirnov test of normality for the d_u terms.

Imaginary part variable FD (d_u)	**T1 CV=0.5102**	**T2 (CV=0.5081)**	**T3 (CV=0.4947)**	**T4 (CV=0.4908)**
D_n	0.197	0.192	0.201	0.203

©2006-2018 Asian Research Publishing Network (ARPN). All rights reserved.

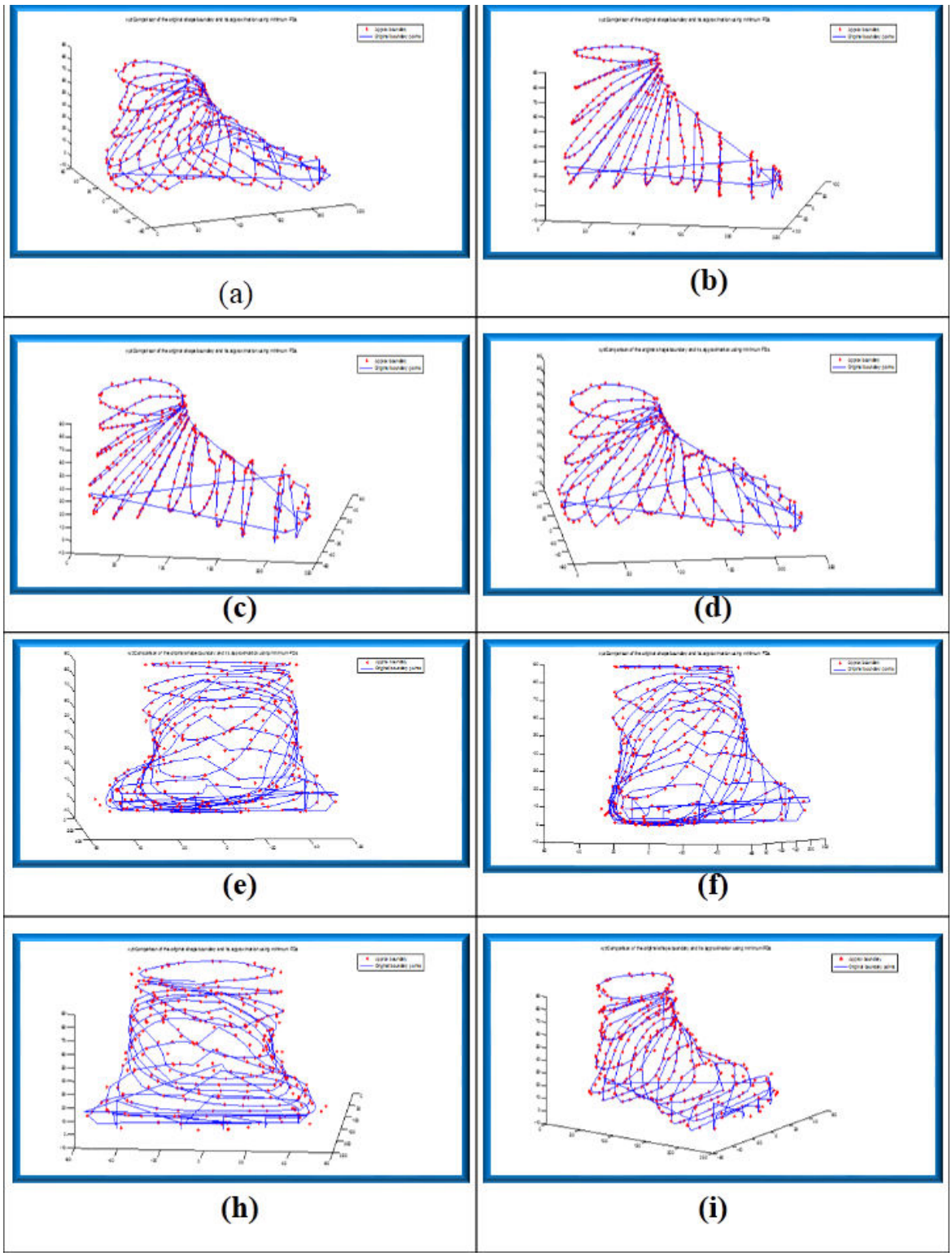

Figure-11. (a)-(h) Different orientation of foot represented by 154 FD model (red points) and 3D homologous model (blue).

The variation of shape

The variation of shape of the foot was obtained and represented by $\mathbf{A}_i$ which is the complex multi-normal probability distribution of $CN(\mu,\Gamma,C)$. Since $\mathbf{A}_i = \mathbf{c}_i + j\mathbf{d}_i$ where $\mathbf{c}_i^T = (c_1, c_2, \ldots, c_{154})$, and $\mathbf{d}_i^T = (d_1, d_2, \ldots, d_{154})$, it is not possible to write $\mathbf{A}_i$ in this paper since it is a very large matrix. The graphical

©2006-2018 Asian Research Publishing Network (ARPN). All rights reserved.

representation of the $\mathbf{A}_i \pm$ SD is given in Figure-12 (a) - (h) showing the mean shape, $\mathbf{A}_i$, in blue color, $\mathbf{A}_i$ + SD in green color and $\mathbf{A}_i$ - SD shape in red color, in different orientation of the foot.

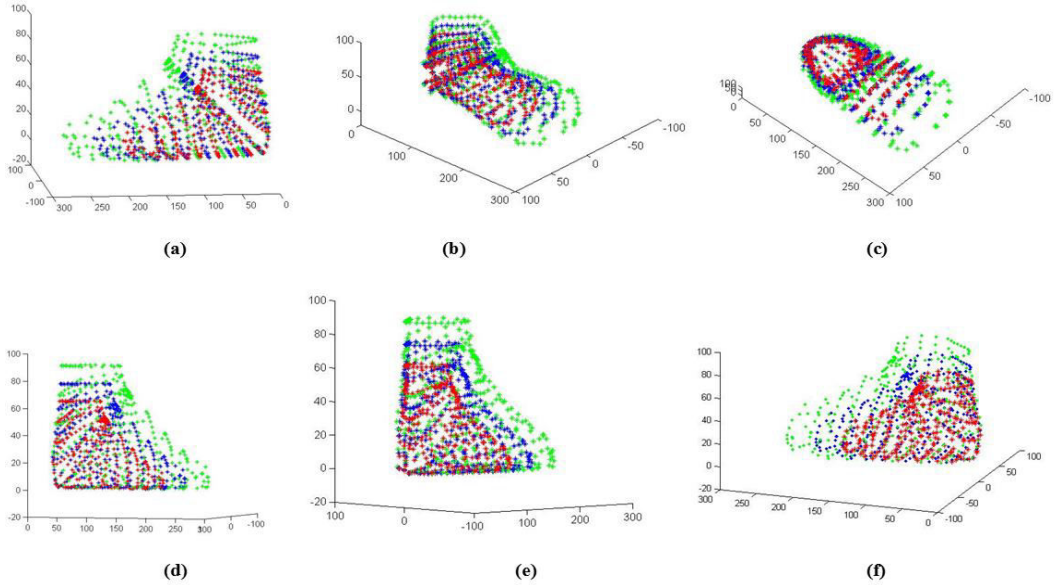

Figure-12. The mean shape A_i shows in blue color, A_i+ SD in green color and A_i- SD shape in red color, in different orientation of the foot.

DISCUSSIONS

Errors in anthropometric measurements are mainly caused by experimental setup during foot scanning. Technical and mechanical limitation of the equipment used for foot scanning will introduce additional errors. In general, such errors will be defined as anthropometric measurement errors (AME). Technical Error of Measurement (TEM) is an indicator to evaluate the data quality, which reflects the performance of the person conducting the measurements (observer) while carrying out the scanning process on the subjects. This TEM indicator verifies the accuracy of the measurement when performing and repeating anthropometrical measurements, adopted by the International Society Standardization Advancement. Accepting low TEM-values and given that the Bland-Altman plots show consistent measurements indicate that the homologous model is accurately obtained. The Procrustes distance was initially used to decide on the number of FD terms where 154 terms were regarded as sufficient. This result was then verified by the similarity indices, Dice similarity Index (D), Jaccard Index (J), volume overlap error (VOE) and relative volume difference (RVD). As an illustration of the similarity between the 3D FD model and the 3D homologous model selected measurements, foot length, foot width, ball girth circumference and foot volume were compared. Both models showed identical univariate measurements whilst the three-dimensional measurement (volume) showed acceptable variation as shown in Table-7 and Table-8 respectively. Incidentally, knowledge of foot length, foot width and ball girth circumference is the minimum number of shape measurements that is required in the Japanese standard system.

A graphical illustration of the appropriateness of the 154 FD model, its 3D representation is overlapped with the corresponding 3D homologous model shown in Figure-12(a) - (h) with different orientation of the foot strongly suggesting that 154 FD model is capable of capturing most of the details of the foot shape. The proposed 154 FD model has numerous applications; firstly, standard shape measurement is easily and efficiently reproduced.

The 154 FD terms was shown to be normally distributed and this implies that the vector of FD terms has a complex normal distribution. The existence of a probability distribution allows further investigation of shape in the form of appropriate hypothesis testing problems.

CONCLUSIONS

A novel robust and invariant foot shape model using Fourier Descriptor is proposed in this study. The proposed model represents foot shape better than using a combination of selected foot dimensions such as foot length, foot width and foot volume widely available from existing foot scanners. This model can nevertheless, derive foot dimensions quickly and accurately, which has important applications in ergonomics. The existence of a probability distribution will enable appropriate hypothesis testing problems to be perform. The proposed model with its properties will be of particular use in the field of ergonomics.

©2006-2018 Asian Research Publishing Network (ARPN). All rights reserved.

ACKNOWLEDGEMENT

The research is funded by University of Malaya research grant (RP004B-13AFR) and the Ministry of Higher Education Malaysia. We wished to thank the contribution from Nurkhairanny Mohktar, Insitute of Mathematical Science research assistant and Prof Makiko Kouchi form Digital Human Research Center, National Institute of Advanced Industrial Science and Technology, Tokyo, Japan.

REFERENCES

[1] Mauch M, Grau S, Krauss I, Maiwald C, Horstmann T. 2008. Foot morphology of normal, underweight and overweight children, International Journal of Obesity (London). 32(7): 1068–1075.

[2] Mauch M, Grau S, Krauss I, Maiwald C, Horstmann T. 2009. A new approach to children's footwear based on foot type classification, Ergonomics. 52(8): 999-1008.

[3] Witana CP, Feng J, Goonetilleke RS. 2004. Dimensional differences for evaluating the quality of footwear fit, Ergonomics. 47(12): 1301-1317.

[4] Ashizawa K, Kumakura C, Kusumoto A, Narasaki S. 1997. Relative foot size and shape to general body size in Javanese, Filipinas and Japanese with special reference to habitual footwear types, Annals of Human Biology. 24(2): 117-129.

[5] Hawes MR, Sovak D. 1994. Quantitative morphology of the human foot in a North American population, Ergonomics. 37(7): 1213-1226.

[6] Fessler DM, Haley KJ, Lal RD. 2005. Sexual dimorphism in foot length proportionate to stature, Annals of Human Biology. 32(1): 44-59.

[7] Mochimaru M, Kouchi M. 1996. Classification of the 3-D foot shape using the Free Form Deformation method, The Japanese Journal of Ergonomics. 32: 68-69.

[8] Krauss I, Grau S, Mauch M, Maiwald C, Horstmann T. 2008. Sex-related differences in foot shape, Ergonomics. 51(11): 1693-1709.

[9] Tierney S, Aslam M, Rennie K, Grace P. 1996. Infrared optoelectronic volumetry, the ideal way to measure limb volume, European Journal of Vascular Endovascular Surgery. 12: 412-417

[10] Hirai M, Iwata H, Niimi K, Koyama A, Komatsubara R. 2012. Improvement of a three dimensional measurement system for the evaluation of foot edema, Skin Research and Technology. 18: 120-124.

[11] Tu HH. 2014. Foot volume estimation formula in healthy adults. International Journal of Industrial Ergonomics. 44: 92-98.

[12] Rossi WA, Tennant R. 1993. Professional shoe fitting, National Shoe Retailer Association, New York, USA.

[13] McWhorter J.W, Wallman. H, Landers. M, Altenburger. B, Laporta-krum. L, Altenburger. P. 2003. The effects of walking, running and shoe size on foot volumetrics, Physical therapy in Sports. 4: 87-92.

[14] Witna CP, Xiong S, Zhao J, Goonetilleke RS. 2006. Foot measurements from three-dimensional scans: A comparison and evaluation of different methods, International Journal industrial Ergonomics. 36: 789-807.

[15] Branthwaite H, Chocklingam N, Greenhalgh A. 2013. The effect of shoe toe box shape and volume on forefoot interdigital and plantar pressures in healthy females, Journal foot Ankle Research. 6: 28-32.

[16] Yu CY and Tu HH. 2009. Foot surface database and estimation formula, Applied Ergonomics. 40: 767-774.

[17] Frey C. 2000. Foot health and shoe wear for women. Clinical Orthopaedics and Related Research. 372: 32-44.

[18] Kouchi M, Mochimaru M, Motoda S. 2013. Evaluation of shoes made using new lasts with modified lateral ball position, Footwear Science. 5: S127-S128.

[19] Kouchi M. 2011. Factors for evaluating high-heeled shoe comfort, Footwear Science. 3: S90-S92.

[20] Yoshida Y, Saito S, Aoki Y, Kouchi M, Mochimaru M. 2012. The Shape completion and modeling of 3D foot shape while walking, International Symposium on Optomechatronic Technologies (ISOT). pp. 1-3.

[21] O'Connor K, Bragdon G, Baumhauer JF. 2006. Sexual dimorphism of the foot and ankle, The Orthopaedic Clinics of North America. 37(4): 569-574.

[22] Voracek M, Fisher ML, Rupp B, Lucas D, Fessler DM. 2007. Sex differences in relative foot length and

©2006-2018 Asian Research Publishing Network (ARPN). All rights reserved.

perceived attractiveness of female feet: Relationships among anthropometry, physique, and preference ratings, Perceptual and Motor Skills. 104(3): 1123-1138.

[23] Zhang D and Lu G. 2001. A comparative study on shape retrieval using Fourier descriptors with different shape signatures, International Conference on Intelligent Multimedia and Distance Education (ICIMADE01). pp. 1-9.

[24] Zhang D and Lu G. 2004. Review of shape representation and description techniques, Pattern Recognition. 37: 1-19.

[25] Dalitz C, Brandt C, Goebbels S, Kolanus D. 2013. Fourier descriptors for broken shapes, EURASIP Journal on Advances in Signal Processing, 161: 1-11.

[26] Zhang D and Lu G. 2002. Shape-based image retrieval using generic Fourier Descriptor, Signal Process.: Image Commun. 17: 825-848.

[27] Arbter K, Snyder W, Burkhardt H, Hirzinger G. 1990. Application of affine-invariant Fourier descriptors to recognition of 3-D objects, Pattern Anal. Mach. Intell. IEEE Trans. 12: 640-647.

[28] Kim H, Kim J. 2000. Region-based shape descriptor invariant to rotation, scale and translation, Signal Process.: Image Commun., 16: 87-93.

[29] ISO 20685:2010. 3-D scanning methodologies for internationally compatible anthropometric databases.

[30] Kouchi M and Mochimaru M. 2011. Errors in landmarking and the evaluation of the accuracy of traditional and 3D anthropometry, Applied Ergonomics. 42: 518-527

[31] Gordon CC, Churchill T, Clauser CE, Bradmiller B, Mc Conville JT, Tebbets I, Walker RA. 1989. Anthropometric Survey of U.S. Army Personnel: Methos and Summary Statistics. Technical Report Natic/TR-89/044.

[32] Bland JM and Altman DG. 1986. Statistical methods for assessing agreement between two methods of clinical measurement. Lancet. 327(8476): 307-10.

[33] Gonzalez RC and Woods RE. 1992. Digital image processing, New York: Addison-Wesley.

[34] Oppenheim AV, Willsky AS, Young I T. 1983. Signals and Systems, Prentice-Hall.

[35] Dryden IL and Mardia KV. 1998. Statistical Shape Analysis, New Jersey: Wiley.

[36] Gower JC and Dijksterhuis GB. 2004. Procrustes Problems, Oxford, UK: Oxford University Press.

[37] Li ZC; Chiang JY, Suen, CY. 2010. Face Transformation With Harmonic Models by the Finite-Volume Method With Delaunay Triangulation, IEEE Trans. Syst, Man, & Cyber. Part B: Cybernetics. 40(6): 1543-1554.

[38] Hogg RV and Tanis EA. 1977. Probability and Statistical Inference, New York: MacMillan.